Chapter 6

Electrochemical detection of dopamine using graphite electrodes modified with PAMAM G4.0-64OH dendrimers in synthetic cerebrospinal fluid

G. Armendariz[1], J. Manríquez[1], A. Santamaría[2], A. Herrera-Gómez[3,4], E. Bustos[1]

[1]Centro de Investigación y Desarrollo Tecnológico en Electroquímica S.C., P.O. Box 064, C.P. 76703, Pedro Escobedo, Querétaro, México.

[2]Instituto Nacional de Neurología y Neurocirugía. Insurgentes Sur No. 3877, México, D.F., C.P. 14269, México.

[3]UAM-Azcapotzalco. Distrito Federal, 02200 México.

[4]CINVESTAV-Unidad Querétaro. Querétaro, Qro. 76230, México.

garmendariz@cideteq.mx, jmanriquez@cideteq.mx, absada@yahoo.com, aherrera@qro.cinvestav.mx, ebustos@cideteq.mx

Doi: http://dx.doi.org/10.3926/oms.122

Referencing this chapter

Armendariz, G., Manríquez, J., Santamaría, A., Herrera-Gómez, A., & Bustos, E. (2014). Electrochemical detection of dopamine using graphite electrodes modified with PAMAM G4.0-64 OH dendrimers in synthetic cerebrospinal fluid. In M. Stoytcheva & J.F. Osma (Eds.). *Biosensors: Recent Advances and Mathematical Challenges*. Barcelona: España, OmniaScience. pp. 129-140.

1. Introduction

Parkinson's disease (PD) is a degenerative disease of the central nervous system which is characterized by the trembling of the arms and legs, stiffness and rigidity of the muscles, and slow movements. PD is one of many diseases related to changes in dopamine (DA) levels, as a deficiency of this neurotransmitter in the basal ganglia is known to play a critical role in this disorder (Ezquerro, 2008; Stella & Rajewski, 1997). DA acts as a messenger in different areas of the brain for coordination of body movements. Accordingly, the main pathological symptom of PD is the selective loss of dopaminergic neurons in the substantia nigra (Stella & Rajewski, 1997). Therefore, new and improved methods for the detection and quantification of DA, which should be immediately useful for basic research and quickly adaptable for clinical purposes, are needed to better understand the pathology and possible treatments of this disease.

Currently, methods based on fluorimetry (Venton & Wightman, 2003; Lin, Qiu, Yang, Cao & Jin, 2006), radioenzymatic assays (Wassell, 1999) and chromatography (Lin et al., 2006, Bergquist, Sciubisz, Kaczor & Silberring, 2002; Peaston & Weinkove, 2004), among others, are commonly used to assess DA. However, electrochemical sensors can also quickly and inexpensively detect DA in CSF, both *in vitro* and *in vivo*. Recent articles have used different electrodes for *in vivo* measurements, although most of them employing carbon-like materials (Venton & Wightman, 2003; Lin et al., 2006; Yavich & Tiihonen, 2000; De Toledo, Santos, Cavalheiro & Mazo, 2005; Qiao, Ding & Wang, 2005; Budai, Gulya, Mészáros, Hernándi & Bali, 2010). Nevertheless, electrode design and construction can still be improved with three highly desirable adjustments: (i) smaller size for easier *in vivo* use, (ii) portability, and (iii) construction of an easy-to-use device that detects and quantifies dopamine in real time.

Previous studies note that treating carbon surfaces with oxidizing agents in gas or liquid phases results in partial surface oxidation (i.e., the formation of oxygen-containing surface functional groups) (Boehm, 1994, 2002; Barton, Evans, Halliop & Macdonald, 1997). Nitric acid, sulfuric acid, and other oxidizing media, such as ozone or oxygen plasma, are also highly effective (Ajayan, Ebbesen, Ichihashi, Ijima, Tanigaki & Hiura, 1993; Kooi, Schlecht, Burghed & Kern, 2002; Hiura, Ebbesen & Tanigaki, 1995; Banerjee, Hemraj-Benny & Wong, 2005; Klein, Melechko, McKnight, Retterer, Rack, Fowlkes et al., 2008). Molecular oxygen only attacks the basal planes of the graphite at peripheries or at defective sites such as edge planes and vacancies (Radovic, 2003; Boehm, 1966; Anderson, 1975).

After treatment, several functional groups on the carbon-like surface, such as carboxyls, carboxylic anhydrides, and lactones, are generally present (Toebes, van Heeswijk, Bitter, van Dillen, de Jong, & de Jong, 2004; Ros, van Dillen, Geus & Koningsberger, 2002; Xia, Su, Birkner, Ruppel, Wang, Woell et al., 2005; Martínez, Callejas, Benito, Cochet, Seeger, Anson et al., 2003). Hydroxyl groups at the edge of graphitic planes exhibit phenolic character, while carbonyl groups, like quinones, remain isolated, or are arranged like pyrones. *Furthermore, both ether oxygens and pyrans can substitute one carbon atom at the edge, and a*ldehydes can also be present on the oxidized carbon surfaces (Kundu, Wang, Wei & Muhler, 2008).

Several experimental techniques, such as acid-base titration (Boehm, 1966, 1994, 2002), infrared spectroscopy (IR) (Ros et al., 2002; Martínez et al., 2003; Fanning & Vannice, 1993; Kastner, Pichler, Kuzmany, Curran, Blau & Weldon, 1994), temperature-programmed desorption (TPD) (Ros et al., 2002; Xia et al., 2005; Haydar, Moreno-Castilla, Ferro-Garcia, Carrasco-Marin, Rivera-Utrilla, Perrard et al., 2000; Zhou, Sui, Zhu, Li, Chen, Dai et al., 2007), and X-ray

photoelectron spectroscopy (XPS) (Martínez et al., 2003; Okpalugo, Papakonstantinou, Murphy, McLaughlin & Brown, 2005; LakshminAeayanan, Toghiani & Pittman, 2004; Park, MaClain, Tian, Suib & Karwacki, 1997), can identify which oxygen functional groups are present on these oxidized carbon-like surfaces. Indeed, XPS can also correctly identify and quantify oxygen-containing functional groups from a variety of carbon materials (Toebes et al., 2004; Kundu et al., 2008; Okpalugo et al., 2005; LakshminAeayanan et al., 2004).

Due to the aforementioned need for new and improved methods of DA detection, we have designed, constructed and characterized a portable electrochemical device which detects and quantifies DA in CSF by using the dendrimer-modified pencil lead graphite (G).

2. Experimental procedure

2.1. Reactives

D-glucose (99.005%), KCl (99.6%), NaF (99.9%), HCl (38% w), $K_3Fe(CN)_6$ (99%), $K_4Fe(CN)_6$ (99%) and H_2SO_4 (97.3%) were obtained from J.T.Baker. $CaCl_2*2H_2O$ (99.0%), NaCl (99.0%), NaOH (97.0%) and $MgSO_4*7H2O$ (98.0%) were obtained from Karal. NaH_2PO_4 (98.0%) was obtained from Reprofiquin, DA (99.9%) from Sigma Chemical Co. (St. Louis, MO, USA) and Generation 4.0 PAMAM dendrimers (–OH terminal groups) from Aldrich.

The 10 mM DA standard stock solution used for DA determination was prepared in phosphate buffer (pH = 7.2, i = 0.1). Synthetic cerebrospinal fluid (SCF) was prepared as follows: 124 mM NaCl, 26 mM $NaHCO_3$, 10 mM D-glucose, 5 mM KCl, 2 mM $MgSO_4*7H_2O$, 1.09 mM NaH_2PO_4, and 1.34 mM $CaCl_2*6H_2O$.

2.2. Construction of the G–PAMAM electrode

A commercial brand of pencil lead (G, ϕ = 0.5 mm, 5 mm length) was electrochemically treated in a 0.5 M H_2SO_4 solution, and 0.6 V vs. Ag/AgCl was applied for 5 min to preferentially promote quinone on the electrode surface (García, Armendáriz, Godínez, Torres, Sepúlveda-Guzmán & Bustos, 2011; Bustos, García, Díaz-Sánchez, Juaristi, Chapman & Godínez, 2007). While similar pre-treatment procedures were recently reported by Bustos and col (García et al., 2011; Bustos et al., 2007), their use of higher potentials promoted other functional groups, such as carboxylic acid (1.6 V vs Ag/AgCl) and phtalic anhydride (2.2 V vs Ag/AgCl).

The pre-treated electrode (G-PF) was rinsed with Milli-Q water. 20 μM PAMAM dendrimer G4.0-64 OH was deposited on the electrode surface by immersion in 0.1 M NaF solution, and application of 0.6 V vs. Ag/AgCl for 1 h, as previously reported (García et al., 2011; Bustos et al., 2007).

2.3. Electrochemical characterization of naked and modified electrodes

Prior to each electrochemical experiment, the electrolytic solutions were deoxygenated by bubbling through ultra-pure nitrogen (PRAXAIR, grade 5.0) for at least 10 min. In addition, all pencil lead were inserted into Transferpette micropipettes tips, sealed with a butane gas flame and rinsed with Milli-Q water before use.

A BAS-Zahner potentiostat was used to perform electrochemical impedance spectroscopy. In the three-electrode system, platinum wire (0.32 cm^2) was the counter electrode and Ag/AgCl (3 M

NaCl), the reference electrode. In the two-electrode system, these electrodes were replaced by a silver wire that had recently been coated with silver chloride and rinsed with water.

To estimate the relative fractional coverage of the surface by the dendrimer, EIS measurements were performed on the modified G-PAMAM electrodes. A 10 mV amplitude wave was used around the equilibrium potential of the 0.1 M KCl solution containing the $Fe(CN)_6^{3-/4-}$ redox couple and the 1 mM $K_3Fe(CN)_6$ electroactive probe. Frequencies from 0.1 Hz to 100 kHz were applied, and impedance values were recorded at 500 discrete frequencies per decade. The charge-transfer resistance, R_{CT}, and the double layer capacitance, C_{DL}, were obtained by fitting the experimental impedance data to Randle's equivalent-circuit model, included in the BAS-Zahner software. EIS was also employed to determine the electroactive area of the graphite electrode in the 0.9 N NaF solution. After the spectra were obtained, an additional capacitance (C_f) was added to a similar equivalent-circuit model, to account for a possible accumulation of fluorine ions between graphene sheets.

Once the electrochemical impedance spectra of the electrodes in NaF solution were obtained and fitted to the equivalent-circuit model mentioned before, total capacitance was determined with the specific capacitance of graphite (0.6 μF cm^{-2}) to calculate the electroactive area (McCreery & Bard, 1991).

On other hand, to estimate the effective fractional coverage of the dendrimer on the graphite surface, impedance analyses in the presence of an electroactive probe were performed. The resulting Nyquist plots were fitted to the equivalent circuit and the fraction of the surface blocked by adsorbed dendrimer was calculated from Equation 1 (Bustos et al., 2007; Tokuhisa, Zhao, Baker, Phan, Dermody, García et al., 1998):

$$\theta = (R_{CT} - R^0_{CT}) / R_{CT} \quad (1)$$

where R^0_{CT} is the charge-transfer resistance for the electroactive probe molecule reaction measured on the bare graphite electrode and R_{CT} the resistance on the coated electrode. This equation, employed in previous papers, assumes that the heterogenous surface is composed of a fractional area that fully blocks electron transfer (θ) and a fractional area that is completely accesible to the probe molecule (1–θ) (Bustos et al., 2007; Tokuhisa et al., 1998).

2.4. Electrochemical detection of Dopamine

Amperometric and voltamperometric measurements were carried out using a BASi Epsilon potentiostat. The current intensities employed in constructing the DA amperometric calibration curves were obtained by measuring the faradaic current of the chronoamperometric measurements. First, consecutive additions of 2 μL DA stock solution were made to a 10 mL cell containing CSF; then, the faradaic current density was measured 30 seconds after running the experiment. Detection (DL) and quantification limits (QL) were calculated using the following equations:

$$DL = 10\sigma/m \quad (2)$$

$$QL = 5\sigma/m \quad (3)$$

where σ is the standard deviation and m is the slope related with the sensitivity of the calibration curve.

2.5. Spectroscopical characterization of naked and modified electrode

The electrodes were then characterized by Raman spectroscopy and X-ray photoinduced spectroscopy (XPS). Raman spectroscopy was performed using a Thermo micro-Raman spectrometer with a 780 nm laser, and XPS using a ThermoFisher-VG instrument equipped with a monochromatic Al Kα1 (1486.7 eV) X-ray source (model XR5) and a hemispherical electron analyzer with seven channeltrons (model XPS110).

3. Results and Discussion

3.1. Characterization of naked and modified graphite electrode

Using the specific capacitance of graphite (0.6 μF cm^{-2}), the electroactive area of graphite electrode was calculated which was around 1.57 cm^2. Later, the rugosity factor (η) of a bare graphite lead electrode was verified by varying the exposure length from 2 to 8 mm. As the expose length increased, electroactive area and total capacitance ($C_T = C_{DL} + C_f$) also increased. Using the correlated increase in C_T and in electroactive area (A_e), the following equation was derived considering the geometric area (A_g):

$$A_e = n\, A_g \tag{4}$$

Plotting the calculated electroactive area (A_e) vs the geometric area (A_g) of the electrode resulted in a linear equation with a slope of 19.85 (A_e = 19.85A_g-0.03; r^2 = 0.9897), where the slope calculated represents η. These results show that the composition of the electrode substrate was constant in the measured interval, leading to a possible miniaturization of the electrode. The resulting fractional coverage (θ = 0.18) shows that nucleophilic attachment of the dendrimer to the electrode surface is slight. The esther-like bonds that are formed between the peripheral O atoms of PAMAM G4.0-64OH dendrimers and the O atoms of phtalic anhydride on the graphite surface could explain the low coverage, with only quinone-favored groups avaliable to act as spacers.

To verify surface transformations after electrochemical pre-treating, XPS measured the composition of the graphite electrode after oxidation in sulfuric acid. XPS spectra of a bare graphite electrode were obtained for the C 1s, Ca 2p and O 1s peaks. The peaks present in the C 1s spectra of both electrodes (Figure 1) are listed in Table 1. Each peak was assigned to a chemical species by using previously reported studies (Kundu et al., 2008); the peaks for the graphite carbon bond at 284.8 eV and the phenol / ether carbon-oxygen single bond (i.e., C-O) at 285.8 eV were present. However, the peak for the ketone / quinone carbon-oxygen double bonds (i.e., C=O) at 286.7 eV and the peak for the carboxyl / carboxylic anhydride / ester carbon bound to two oxygens (i.e.; -COO) at 287.6 eV were only seen in the pre-treated graphite electrodes. Finally, a significant decrease in the C-O peak shows that the pre-treatment of the surface successfully partially oxidized hydroquinone, creating quinone functional groups.

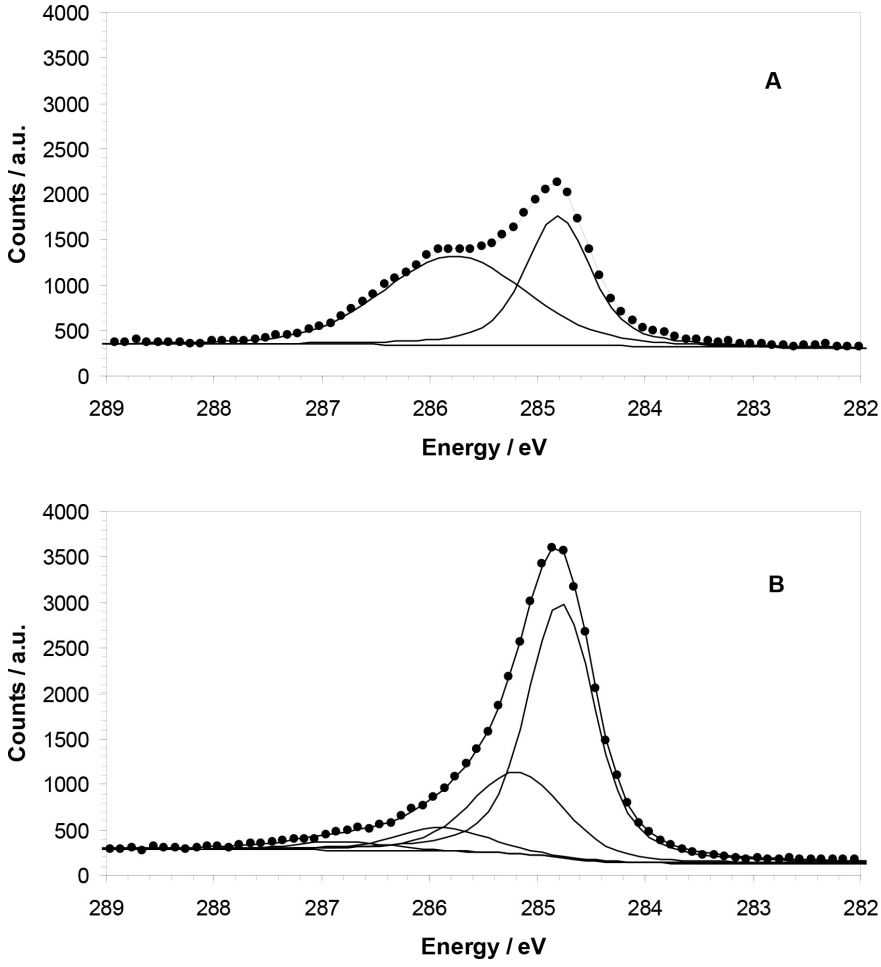

Figure 1. C 1s XPS spectra of a bare graphite electrode (A) naked and (B) pre-functionalized. The constituting peaks corresponding to each chemical species are also shown

Electrode	Bounding Energy / eV	Assignment	Area / a.u.	Electrode	Bounding Energy / eV	Assignment	Area / a.u.
G	284.8	C=C	1259.3	G-PF	284.8	C=C	3017.52
	285.8	C-O	1876.3		285.4	C-O	717.84
	286.7	C=O	0		286.7	C=O	297.83
	287.6	-COO	0		287.6	C-O	150.34

Table 1. Relative areas determined from deconvoluted XPS spectra of bare (G) and pre-treated (G-PF) graphite electrode

Figure 2 shows the typical Raman spectra of G (a), G-PF (b) and G-PAMAM (c). The peaks at 1360 cm^{-1} (D band) and 1580 cm^{-1} (G band) have been seen in several previous studies. The G band was assigned to the E_{2g} vibrational mode, only possible in sp^2 graphite, and the D band to the loss of symmetry along the microcrystal, like in the edges of graphene sheets (Tuinstra & Koenig, 1970). The change in the D band suggests that the number of defects in the graphite increases (from 24.50 to 41.21) when PAMAM dendrimers are coated onto the graphite surface

(Table 2). On the other hand, the increase of the G band (from 22.51 to 36.89) is most likely due to the increase of sp^2 carbon from the dendrimer branches. The lack of change in relative intensities of the D and G bands (i.e., I_D / I_G) provides evidence of edge-plane exposure. The values of I_D / I_G for all samples are similar, probably due to the low coverage of the dendrimer on the graphite surface in G-PAMAM electrodes (θ = 0.18). Furthermore, I_D / I_G ratios obtained in this study are similar to those reported by Liu (I_D / I_G = 1.4) for carbon fiber electrodes employed in the simultaneous detection of dopamine, uric acid and ascorbic acid (Liu, Huang, Hou & You, 2008).

Electrode	I_D	I_G	I_D / I_G
G	24.50	22.51	1.09
G – PF	25.33	23.00	1.10
G - PAMAM	41.21	36.89	1.12

Table 2. D (I_D) and G (I_G) band relative intensities of the electrodes, obtained from Raman spectra

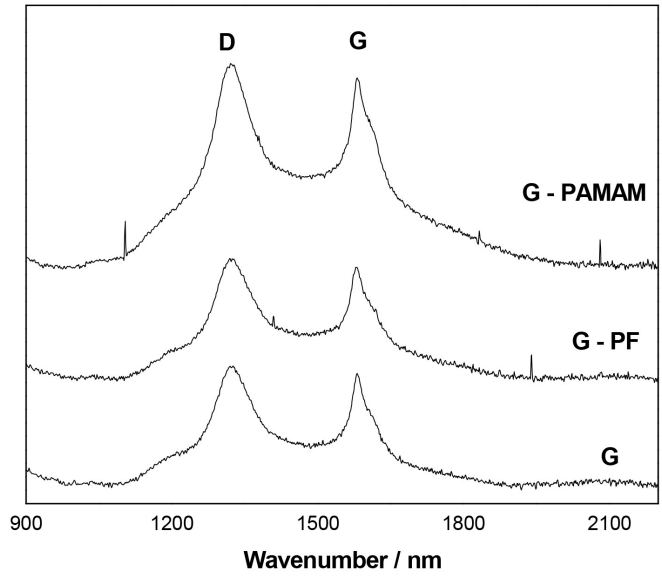

Figure 2. Raman spectra of the bare (G), the pre-treated (G-PF) and the modified electrode(G-PANAM)

3.2. Electrochemical response of dopamine using naked and modified graphite electrode

The electrochemical response of DA was examined by cyclic voltammetry (CV), using bare (A), pretreated (B), and modified (C) graphite electrodes in a three-electrode cell (Figure 3). For these experiments, a fresh 10 μM DA solution in CSF was prepared. The oxidation peak charge of DA (for the reaction DA-$2e^-$ → DOQ + $2H^+$) obtained using G-PAMAM (1.38 μC) is much greater than those obtained using G (0.59 μC) and G-PF (0.64 μC). The increase in oxidation peak charge and the change in the shape of the voltamperogram indicates that dendrimers coated on the electrode's surface could enhance the sensitivity of the electrode. Later, the system was simplified by replacing the reference and counter electrode with a silver wire (0.32 cm^2) coated with silver chlorine. Since the composition of SCF is sufficiently high in chlorine, the electrode itself acts as an ideal non-polarizable electrode, guaranteeing accurate measurement. CV

verified this asservation (Figure 4) by comparing a two-electrode (A) and three-electrode system (B) in 10µM DA solution. Though the oxidation potential of DA differed when using different electrode systems, current intensity remained constant for both. Therefore, the following experiments were carried out in a two-electrode cell.

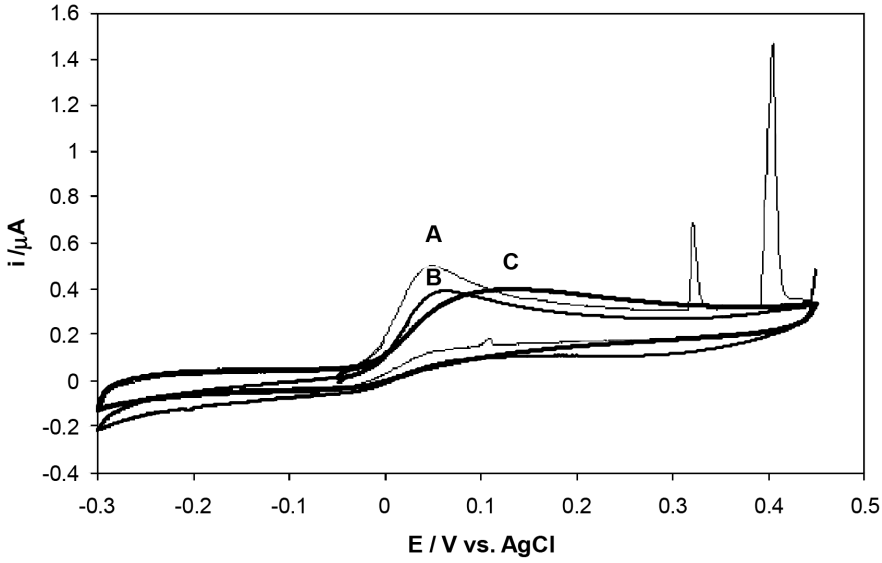

Figure 3. CVs of G (A), G – PF (B) and G – PAMAM (C) electrodes in 10 µM DA in CSF, v = 20 mV s^{-1} using three-electrode system

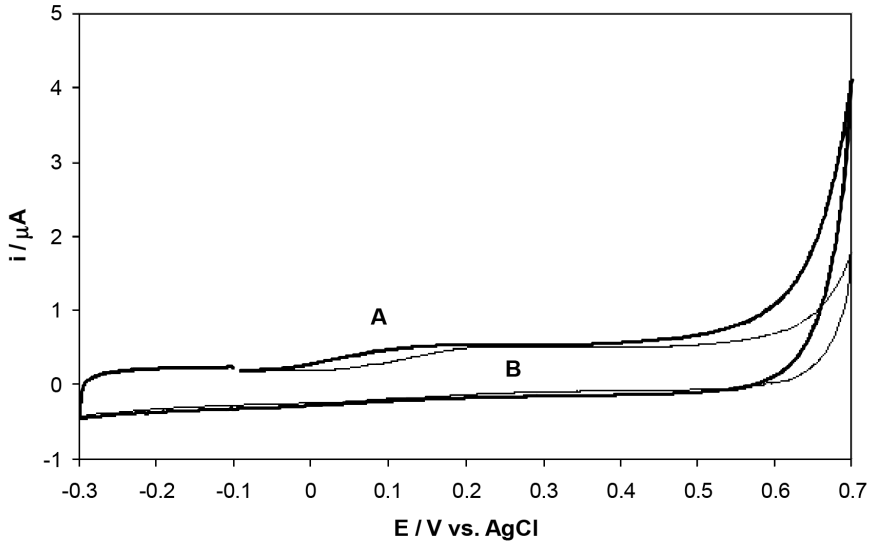

Figure 4. CV of a two (A) and a three (B) electrode system in 10 µM DA in CSF, v = 20 mV s^{-1} using a modified electrode with G-PAMAM

3.3. Calibration curves for dopamine using naked and modified graphite electrode

A two-electrode system was employed to create calibration plots for dopamine, using DA concentrations from 0 to 20 µM. As Figure 5 shows, in this concentration range, the G-PAMAM electrode shows greater sensitivity than the bare electrode (Table 3). Although the increase in sensitivity was slight, the standard deviation of data in the absence of analyte (σ) greatly differed (by a factor of 46), greatly improving DL and QL for this electrode. In fact, according to these results, it is possible to detect 6.67 nM and quantify 22.24 nM of DA using a pencil lead graphite electrode modified with PAMAM G4.0-64OH dendrimers.

Electrode	Sensitivity ($\mu A\ \mu M^{-1}$)	DL (nM)	QL (nM)	Equation (i [=] µA; C [=] µM)	r^2
G	0.0091	306.25	1020.84	i = 0.0091[C] + 0.208	0.987
G – PF	0.0101	37.50	124.99	i = 0.0101[C] + 0.115	0.995
G - PAMAM	0.0187	6.67	22.23	i = 0.0187[C] + 0.001	0.997

Table 3. Detection (DL) and quantification limits (QL) for the electrochemical detection of DA in CSF, using G, G-PF and G-PAMAM electrodes

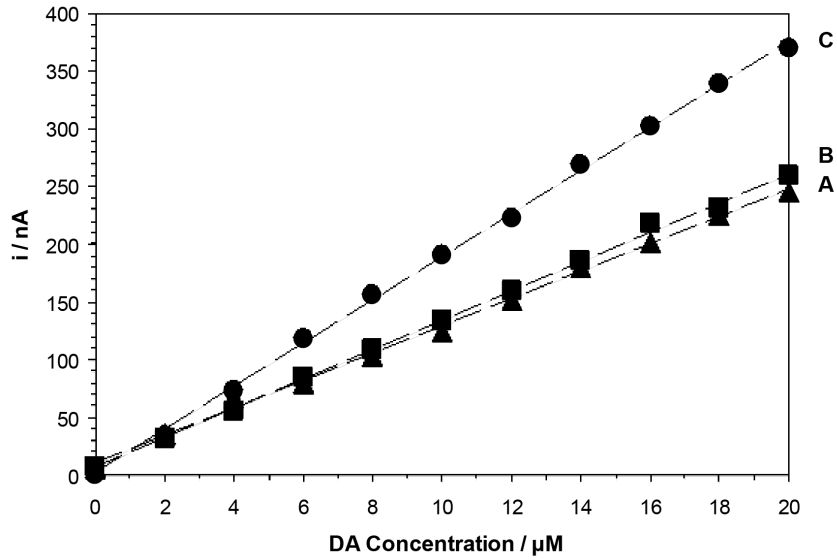

Figure 5. Amperometric calibration plots of DA in CSF using G (A), G-PF (B) and G-PAMAM (C) electrodes

4. Conclusions

Graphite pencil lead electrodes modified with PAMAM G4.0-64OH dendrimers (G-PAMAM) show good performance in detecting DA in SCF. This modified electrode was characterized by spectroscopic techniques and retained 18% of the electrode's relative surface coverage. In addition, the 3-electrode system was simplified to a 2-electrode system. Calibration plots show that the modified electrode detects and quantifies up to 6.67 nM and 22.24 nM, respectively.

Acknowledgment

The authors would like to thank the Consejo Nacional de Ciencia y Tecnología de los Estados Unidos Mexicanos (CONACyT), the Fondo Mixto del Estado de Veracruz Ignacio de la Llave (FOMIX-Veracruz), the Fondo de Cooperación Internacional de Ciencia y Tecnología Unión Europea-México (FONCICyT) ALA/2006/18149, Professor Tessy López and Prof. Yunny Meas Vöng for the funding of this research. The authors also want to thank to Lucy Yao, Peace Corps volunteer at CIDETEQ for her English revision of this manuscript.

References

Ajayan, P.M., Ebbesen, T.W., Ichihashi, T., Ijima, S., Tanigaki, T., & Hiura, H. (1993). Opening carbon nanotubes with oxygen and implications for filling. *Nature, 362*, 522-525. http://dx.doi.org/10.1038/362522a0

Anderson, J.R. (1975). *Structure of Metallic Catalysts.* U.S.: Academic Press Inc.

Banerjee, S., Hemraj-Benny, T., & Wong, S.S. (2005). Covalent surface chemistry of single-walled carbon nanotubes. *Advanced Materials, 17(1)*, 17-29. http://dx.doi.org/10.1002/adma.200401340

Barton, S.S., Evans, M.J.B., Halliop, E., & Macdonald, J.A.F. (1997). Acidic and basic sites on the surface of porous carbon. *Carbon, 35(9)*, 1361-1366. http://dx.doi.org/10.1016/S0008-6223(97)00080-8

Bergquist, J., Sciubisz, A., Kaczor, A., & Silberring, J. (2002). Catecholamines and methods for their identification and quantification in biological tissues and fluids. J*ournal of Neuroscience Methods, 113(1)*, 1-13. http://dx.doi.org/10.1016/S0165-0270(01)00502-7

Boehm, H.P. (1966). Chemical identification of surface groups. *Advanced Synthesis and Catalysis, 16*, 179-274.

Boehm, H.P. (1994). Some aspects of the surface chemistry of carbon blacks and other carbons. *Carbon, 32*, 759-769. http://dx.doi.org/10.1016/0008-6223(94)90031-0

Boehm, H.P. (2002). Surface oxides on carbon and their analysis: a critical assessment. *Carbon, 40*, 145-149. http://dx.doi.org/10.1016/S0008-6223(01)00165-8

Budai, D., Gulya K., Mészáros, B., Hernándi, I., & Bali, Z.K. (2010). Electrochemical responses of carbon fiber microelectrodes to dopamine in vitro and in vivo. *Acta Biologica Szegediensis, 54(2)*, 155-160.

Bustos, E., García, M.G., Díaz-Sánchez, B.R., Juaristi, E., Chapman, Th.W., & Godínez, L.A. (2007). Glassy carbon electrodes modified with composites of starburst-PAMAM dendrimers containing metal nanoparticles for amperometric detectionof dopamine in urine. *Talanta, 72(4)*, 1586-1592. http://dx.doi.org/10.1016/j.talanta.2007.02.017

De Toledo, R.A., Santos, M.C., Cavalheiro, E.T.G., & Mazo, L.H. (2005). Determination of dopamine in synthetic cerebrospinal fluid by SWV with a graphite-polyurethane composite electrode. *Analytical and Bioanalytical Chemistry, 381(6)*, 1161-1166. http://dx.doi.org/10.1007/s00216-005-3066-y

Ezquerro, M. (2008). Investigación en enfermedades neurodegenerativas. Evitando la epidemia "silenciosa" del siglo XXI. *Enfermería Global, 14(1)*, 1-10.

Fanning, P.E., & Vannice, M.A. (1993). A DRIFTS study of the formation of surface groups on carbon by oxidation. *Carbon, 31(5)*, 721-722. http://dx.doi.org/10.1016/0008-6223(93)90009-Y

García, M.G., Armendáriz, G.M.E., Godínez, L.A., Torres, J., Sepúlveda-Guzmán, S., & Bustos, E. (2011). Detection of dopamine in non-treated urine samples using glassy carbon electrodes modified with PAMAM dendrimer-Pt composites. *Electrochimica Acta, 56(22)*, 7712-7717. http://dx.doi.org/10.1016/j.electacta.2011.06.035

Haydar, S., Moreno-Castilla, C., Ferro-Garcia, C., Carrasco-Marin, F., Rivera-Utrilla, J., Perrard, J., et al. (2000). Regularities in the temperature-programmed desorption spectra of CO2 and CO from activated carbons. *Carbon, 38(9)*, 1297-1308. http://dx.doi.org/10.1016/S0008-6223(99)00256-0

Hiura, H., Ebbesen, T.W., & Tanigaki, T. (1995). Opening and purification of carbon nanotubes in high yields. *Advanced Materials, 7(3)*, 275-276. http://dx.doi.org/10.1002/adma.19950070304

Kastner, J., Pichler, T., Kuzmany, H., Curran, S., Blau, W., & Weldon, D.N. (1994). Resonance Raman and infrared spectroscopy of carbon nanotubes. *Chemical Physics Letters, 221(1-2)*, 53-58. http://dx.doi.org/10.1016/0009-2614(94)87015-2

Klein, K.L., Melechko, A.V., McKnight, T.E., Retterer, S.T., Rack, P.D., Fowlkes, J.D., et al. (2008). Surface characterization and functionalization of carbon nanofibers. *Journal of Applied Physics, 103*, 103. http://dx.doi.org/10.1063/1.2840049

Kooi, S.E., Schlecht, U., Burghed, M., & Kern, K. (2002). Electrochemical modification of single carbon nanotubes. *Angewandte Chemie International Edition, 41(8)*, 1353-1355. http://dx.doi.org/10.1002/1521-3773(20020415)41:8<1353::AID-ANIE1353>3.0.CO;2-I

Kundu, S., Wang, Y.M., Wei, X., & Muhler, M. (2008) Thermal stability and reducibility of oxygen-containing functional groups on multiwalled carbon nanotube surfaces: a quantitative high-resolution XPS and TPD / TPR study. *The Journal of Physical Chemistry, 112(43)*, 16869-16878.

Lakshminarayanan, P.V., Toghiani, H., & Pittman, C.U. (2004). Nitric acid oxidation of vapor grown carbon nanofibers. *Carbon, 42(12-13)*, 2433-2442. http://dx.doi.org/10.1016/j.carbon.2004.04.040

Lin, L., Qiu, P.H., Yang, L.Z., Cao, X.N., & Jin, L.T. (2006). Determination of dopamine in rat striatum by microdialysis and high-performance liquid chromatography with electrochemical detection on a functionalized multi-wall carbon nanotube electrode. *Analytical and Bioanalytical Chemistry, 384(6)*, 1308-1313. http://dx.doi.org/10.1007/s00216-005-0275-3

Liu, Y., Huang, J., Hou, H., & You, T. (2008). Simultaneous determination of dopamine, ascorbic acid and uric acid with electrospun carbon nanofibers modified electrode. *Electrochemistry Communications, 10,* 1431-1434. http://dx.doi.org/10.1016/j.elecom.2008.07.020

Martinez, M.T., Callejas, M.A., Benito, A.M., Cochet, M., Seeger, T., Anson, A., et al. (2003). Sensitivity of single wall carbon nanotubes to oxidative processing: structural modification, intercalation and functionalisation. *Carbon, 41(12)*, 2247-2256. http://dx.doi.org/10.1016/S0008-6223(03)00250-1

McCreery, R.L., & Bard, A.J. (Eds.). (1991). *Electroanalytical Chemistry.* New York, U.S.: Dekker.

Okpalugo, T.I.T., Papakonstantinou, P., Murphy, H., McLaughlin, J., & Brown, N.M.D. (2005). High resolution XPS characterization of chemical functionalized MWCNTs and SWCNTs. *Carbon, 43(1)*, 153-161. http://dx.doi.org/10.1016/j.carbon.2004.08.033

Park, S.H.P., MaClain, S., Tian, Z.R., Suib, S.L., & Karwacki, C. (1997). Surface and bulk measurements of metals deposited on activated carbon. *Chemistry of Materials, 9(1),* 176-183. http://dx.doi.org/10.1021/cm9602712

Peaston, R., & Weinkove, C. (2004). Measurement of catecholamines and their metabolites. *Annals of Clinical Biochemistry, 41(1),* 17-38. http://dx.doi.org/10.1258/000456304322664663

Qiao, X., Ding, H., & Wang, Z.F. (2005). Preparation of micro-biosensor and its application in monitoring in vivo change of dopamine. *Journal of Huazhong University of Science and Technology, 25(1)*, 107-108. http://dx.doi.org/10.1007/BF02831402

Radovic, L.R. (2003). *Chemistry and Physics of Carbon.* New York: Marcel Dekker Inc.

Ros, T.G., van Dillen, A.J., Geus, J.W., & Koningsberger, D.C. (2002). Surface oxidation of carbon nanofibres. *Chemistry-A European Journal, 8(5)*, 1151-1162. http://dx.doi.org/10.1002/1521-3765(20020301)8:5<1151::AID-CHEM1151>3.0.CO;2-#

Stella, V. J., & Rajewski, R. A. (1997). Cyclodextrins: their future in drug formulation and delivery. *Pharmaceutical Research, 14(5)*, 556-557. http://dx.doi.org/10.1023/A:1012136608249

Toebes, M.L., van Heeswijk, J.M.P., Bitter, J.H., van Dillen, A.J., de Jong, & de Jong, K.P. (2004). The influence of oxidation on the texture and the number of oxygen-containing surface groups of carbon nanofibers. *Carbon, 42(2)*, 307-315. http://dx.doi.org/10.1016/j.carbon.2003.10.036

Tokuhisa, H., Zhao, M., Baker, L.A., Phan, V.T., Dermody, D.L., García, M.E., et al. (1998). Preparation and characterization of dendrimer monolayers and dendrimer-alkanethiol mixed monolayers adsorbd to gold. *Journal of the American Chemical Society, 120(18)*, 4492-4501. http://dx.doi.org/10.1021/ja9742904

Tuinstra, F., & Koenig, J.L. (1970). Raman spectrum of graphite. *Journal of Chemical Physics, 53(3)*, 1126-1130. http://dx.doi.org/10.1063/1.1674108

Venton, B., & Wightman, M. (2003). Psychoanalytical electrochemistry: dopamine and behavior. *Analytical Chemistry, 75(19)*, 414A-421A. http://dx.doi.org/10.1021/ac031421c

Wassell, J. (1999). Freedom from drug interference in new immunoassays for urinary catecholamines and metanephrines. *Clinical Chemistry, 45(12)*, 2216-2223.

Xia, W., Su, D., Birkner, A., Ruppel, L., Wang, Y., Woell, Q.J., et al. (2005). Chemical vapor deposition and synthesis on carbon nanofibers: sintering of ferrocene-derived supported iron nanoparticles and the catalytic growth of secondary carbon nanofibers. *Chemistry of Materials, 17(23)*, 5737-5742. http://dx.doi.org/10.1021/cm051623k

Yavich, L., & Tiihonen, J. (2000). In vivo voltammetry with removable carbon fibre electrodes in freely-moving mice: dopamine release during intracranial self-stimulation. *Journal of Neuroscience Methods, 104(1)*, 53-63. http://dx.doi.org/10.1016/S0165-0270(00)00321-6

Zhou, J.H., Sui, Z.J., Zhu, J., Li, P., Chen, D., Dai, Y.C., et al. (2007). Characterization of surface oxygen complexes on carbon nanofibers by TPD, XPS and FT-IR. *Carbon, 45(4)*, 785-796. http://dx.doi.org/10.1016/j.carbon.2006.11.019